© 2018. Published by The Company of Biologists Ltd | Journal of Experimental Biology (2018) 221, jeb179242. doi:10.1242/jeb.179242

RESEARCH ARTICLE

Holding tight to feathers – structural specializations and attachment properties of the avian ectoparasite *Crataerina pallida* (Diptera, Hippoboscidae)

Dennis S. Petersen[1,*], Nils Kreuter[1], Lars Heepe[1], Sebastian Büsse[1], Arndt H. J. Wellbrock[2], Klaudia Witte[2] and Stanislav N. Gorb[1]

ABSTRACT

The louse fly *Crataerina pallida* is an obligate blood-sucking ectoparasite of the common swift *Apus apus*. As a result of reduction of the wings, *C. pallida* is unable to fly; thus, an effective and reliable attachment to their host's plumage is of utmost importance. The attachment system of *C. pallida* shows several modifications in comparison to that of other calyptrate flies, notably the large tridentate claws and the dichotomously shaped setae located on the pulvilli. Based on data from morphological analysis, confocal laser scanning microscopy, cryo-scanning electron microscopy and attachment force experiments performed on native (feathers) as well as artificial substrates (glass, epoxy resin and silicone rubber), we showed that the entire attachment system is highly adapted to the fly's lifestyle as an ectoparasite. The claws in particular are the main contributor to strong attachment to the host. Resulting attachment forces on feathers make it impossible to detach *C. pallida* without damage to the feathers or to the legs of the louse fly itself. Well-developed pulvilli are responsible for the attachment to smooth surfaces. Both dichotomously shaped setae and high setal density explain high attachment forces observed on smooth substrates. For the first time, we demonstrate a material gradient within the setae, with soft, resilin-dominated apical tips and stiff, more sclerotized bases in Diptera. The empodium seems not to be directly involved in the attachment process, but it might operate as a cleaning device and may be essential to maintain the functionality of the entire attachment system.

KEY WORDS: Biomechanics, Interlocking, Friction, Adhesion, Ecomorphology, Parasitism, Pulvilli, Empodium

INTRODUCTION

Louse flies (Diptera: Hippoboscidae) are obligate blood-sucking ectoparasites of mammals and birds (Bequaert, 1953). Therefore, an effective and reliable attachment to their host surface is of utmost importance (Marshall, 1981). The louse fly *Crataerina pallida* (Olivier in Latreille 1811) is a flightless, monoxenous avian ectoparasite of the common swift *Apus apus* (Linnaeus 1758; Kemper, 1951; Oldroyd, 1966) (Fig. 1). The general equipment of *C. pallida*'s attachment system, located at the pretarsus, is similar to that of other calyptrate flies and consists of a paired claw, an empodium and paired pulvilli covered with tenent setae (Kemper, 1951; Whitten, 1969; Gorb, 1998, 2001; Gorb et al., 2012; Beutel and Gorb, 2001; Friedemann et al., 2014; Wang et al., 2016). Similar to Coleoptera, previously widely used as a model system for insect attachment (Stork 1980; Gorb and Gorb, 2002, 2009, 2011; Peressadko and Gorb, 2004; Gorb et al., 2005; Voigt et al., 2008; Bullock and Federle, 2011), calyptrate flies are able to attach to a variety of different smooth and rough substrates. The attachment devices of beetles and flies are covered with tenent setae that enable a reliable attachment to smooth substrates by the combination of capillary and intermolecular van der Waals forces (Langer et al., 2004). Claws are used to mechanically interlock whenever insects encounter rough substrates (Stork, 1983a,b; Dai et al., 2002; Niederegger and Gorb, 2003; Persson, 2003; Song et al., 2016).

Normally, representatives of calyptratae have single-tipped claws. *Craterina pallida*, in contrast, possesses a bidentate claw with a strongly developed blade-like heel. This modification is assumed to be an adaptation for the attachment to feathers of the common swift (Kemper, 1951; Bequaert, 1953).

The majority of previous studies on *C. pallida* focused on its physiology and ecological aspects of the host–parasite interaction (Bequaert, 1953; Hutson, 1981; Lee and Clayton, 1995; Tompkins et al., 1996). However, the attachment device and the underlying mechanisms as well as the ability of the louse fly to attach to its host surface are not well understood. In the present study, we provide a detailed visualization of the tarsal morphology and material composition using cryo-scanning electron microscopy (cryo-SEM) in combination with confocal laser scanning microscopy (CLSM). In order to estimate the attachment ability of *C. pallida* and the functional mechanism of its attachment device, we performed attachment force experiments on native (feathers of *A. apus*) and artificial smooth and structured substrates. The contact between attachment devices of *C. pallida* and feathers was also visualized using cryo-SEM.

MATERIALS AND METHODS

Specimens

The swift louse fly lives in and around nests of the common swift, a colonial cave breeder, sucking blood from adult and juvenile swifts. Mature flies hatch from dormant pupae during the incubation of the swifts at end of May, triggered by ambient temperature. Female louse flies deposit pupae around the swifts' nest, which stay dormant until the next breeding season (Hutson, 1981). Larval development takes place within the mother's body (Lee and Clayton, 1995). Adult louse flies die at the end of the breeding season when swifts depart from their nesting site. Pupae of

[1]Department of Functional Morphology and Biomechanics Zoological Institute, Kiel University, Am Botanischen Garten 1–9, 24098 Kiel, Germany. [2]Research Group of Ecology and Behavioral Biology, Institute of Biology, Department of Chemistry-Biology, University of Siegen, Adolf-Reichwein-Str. 2, 57076 Siegen, Germany.

*Author for correspondence (dpetersen@zoologie.uni-kiel.de)

D.S.P., 0000-0002-6473-0227

Received 12 February 2018; Accepted 23 April 2018

Journal of Experimental Biology (2018) 221, jeb179242. doi:10.1242/jeb.179242

Fig. 1. The avian ectoparasite *Crataerina pallida* attached to the plumage of the common swift *Apus apus*.

Craterina pallida were collected at a nesting site of *A. apus* located inside a federal highway bridge near Olpe, Germany (51°02′33″N, 7°49′40″E). The pupae were stored for hatching at 10°C. After hatching and following 1 h of cuticle sclerotization, the louse flies were separated into individual plastic tubes and stored at 10°C prior to experiments. The louse flies were sexed on the basis of external characteristics (e.g. shape of the abdomen; Kemper, 1951).

Scanning electron microscopy (SEM)

Several male and female specimens of *C. pallida* were air dried and the tarsi were prepared with a pair of super-fine FST scissors (Fine Science Tools GmbH, Heidelberg, Germany) and then mounted on stubs. The samples were sputter-coated with 20 nm Au-Pd. SEM images were taken with a Hitachi S-4800 (Hitachi High-Technologies Corp., Tokyo, Japan) at an acceleration voltage of 3 kV. Morphometry of the attachment structures was analysed using ImageJ (v2.0.0-rc-43/1.50e, Wayne Rasband, National Institutes of Health, USA).

Visualization of contact formation by *C. pallida* on feathers

The sites of attachment devices of *C. pallida* on feathers were analysed with a Hitachi S-4800 (Hitachi High-Technologies Corp.) equipped with a Gatan ALTO-2500 cryo preparation system (Gatan Inc., Abingdon, UK). Feathers were taken from a common swift which was found dead at the nesting site inside the bridge. The feathers were then glued to a glass substrate with a similar orientation to that observed on the swift. Four living *C. pallida* individuals in contact with feathers were frozen in liquid nitrogen. Then, the samples were transferred onto the cryo-stage (−140°C) of the preparation chamber, sublimated for 2 min at −90°C and sputter coated with 15 nm Au-Pd. All images were captured at a temperature of −120°C and an acceleration voltage of 3 kV.

Confocal laser scanning microscopy (CLSM)

Several specimens of *C. pallida* were stored at −70°C. After dissection, legs were washed in ethanol (70%) and transferred into glycerine (≥99.5%). Subsequently, samples were mounted on a glass slide using glycerine and were covered with a high-precision coverslip. A Zeiss LSM700 confocal laser scanning microscope (Carl Zeiss MicroImaging GmbH, Oberkochen, Germany) equipped with four stable solid-state lasers was used to capture the auto-fluorescence of the material composition. Auto-fluorescence of the soft rubber-like protein resilin was captured with a 405 nm laser line in combination with a bandpass emission filter transmitting 420–480 nm. Auto-fluorescence of more sclerotized parts was captured by the 488 and 555 nm laser lines together with long-pass emission filters transmitting light wavelengths equal to or bigger than 490 and 560 nm. Auto-fluorescence exceeding this range was captured with the 639 nm line in combination with the above-mentioned 560 nm long-pass emission filter. The obtained auto-fluorescence was subsequently processed by maximum intensity projection using the software packages ZEN (Carl Zeiss MicroImaging GmbH), Affinity Photo and Affinity Design (Apple Inc., Cupertino, CA, USA). For detailed information see Michels and Gorb (2012).

Attachment force experiment

Active pulling of louse flies

Twenty-nine specimens of *C. pallida* were attached to the apparatus by gluing a human hair to the thorax of the specimen and linking it to the force transducer (10 g capacity; FORT10, World Precision Instruments, Inc., Sarasota, FL, USA). The force transducer was connected to a BIOPAC TCI-102 system and a BIOPAC Model MP100 (BIOPAC Systems, Inc., Goleta, CA, USA). Force–time curves were recorded from active pulling insects and visualized with the software Acq Knowledge 3.7.0 (BIOPAC Systems, Inc.). The specimens pulled for 30 s and the highest peak of the graph was considered the maximum attachment force.

The specimens were forced to run over an anisotropic or smooth surface in the perpendicular direction with respect to the orientation of the force sensor by poking them with a wooden stick. The anisotropic surfaces (made from epoxy resin and silicone rubber, see ‘Substrate preparation’, below) were aligned in three directions (along, against and lateral to the inclination of surface structures) with respect to the direction of the walking fly. In total, nine measurements including three controls (see ‘Substrate preparation’, below) were performed for each fly. All surfaces were carefully cleaned with isopropyl alcohol prior to the experiment. All experiments were performed at 25°C and 80% humidity.

Pulling of single legs on feathers

Single detached louse fly legs, interlocked with feathers taken from the dorsal tail region of dead *A. apus*, were pulled to estimate the maximum force possible by passive interlocking. Legs were glued to the force sensor connected to a moveable micromanipulator. Feathers of *A. apus* were glued to a glass surface in order to mimic the plumage. The pretarsus was slightly pushed into the feathers to put it in contact with the feathers and then pulled actively against the orientation of the claws.

Substrate preparation

Three types of substrate material were used throughout the experiments: glass, epoxy resin and silicone rubber. Saw teeth structures were used primarily to probe the attachment (interlocking) ability of *C. pallida* to smooth surfaces and were made up of two different materials [epoxy resin and polyvinylsiloxane (PVS)], which varied in stiffness. The two materials varied in stiffness and were used primarily to probe the attachment ability to smooth surfaces. The saw teeth were produced by using a metal master surface as a mould (Tramsen et al., 2018). They had a base diameter of 1 mm with a height of 1.6 mm; the structures were pointed and anisotropically inclined at an angle of 60 deg. For silicone rubber (PVS) substrates, President light body material (Coltene/Whaledent

AG, Altstätten, Switzerland) was used. For epoxy resin substrates, PVS substrates were filled with an epoxy resin compound (Spurr, 1969) and cured at 70°C for 24 h. The saw teeth epoxy resin and PVS substrates were quadratic (5 cm×5 cm). Smooth surfaces made up of glass, epoxy resin and PVS were used as controls. The smooth glass surface used had a profile roughness (R_a) of 0.003 µm and the saw teeth metal master surface had a R_a of 4.200 µm.

Statistical analysis

A two-way ANOVA was performed in order to evaluate the influence of substrate material and topography on the maximum friction force of *C. pallida*. If significant differences were found, a Holm–Sidak *post hoc* test was performed. All statistical analyses were executed using SigmaPlot 12.0 (Systat Software Inc., San Jose, CA, USA). If not stated otherwise, the data was normally distributed and showed homoscedasticity.

RESULTS

Morphology of the attachment system

No specific differences in the attachment system were observed between males and females. Also, no specific differences in the attachment system of the three leg pairs were revealed. In general, the entire attachment system consisted of three parts: one pair of bidentate claws [claw segment 1 (CS1), claw segment 2 (CS2)] with blade-like enlarged heels [claw segment 3 (CS3)], two pulvilli (adhesive pads) located beneath the claws and an empodium located between the two pulvilli (Fig. 2A,C). At their bases, the claws were oval and became more acuminated in the apical direction (Fig. 2B). All three claw segments differed in their width, length and shape. The most apical one (CS1) showed a characteristic acuminated shape and had conspicuous grooves in the dorso-lateral as well as in the ventro-lateral region (Fig. 2A,B). The distance between the base and the tip length of the claw was 626±37 µm (mean±s.d., n=4), making CS1 the longest of all three claw segments. The base diameter was 87±8 µm (n=4).

The above-mentioned grooves were periodically arranged in the dorso-lateral region of the claws (Fig. 2B). They ran obliquely and pointed away from the distal end of the claw. The angles at which the grooves were orientated differed from ∼16 deg at the distal end of CS1 up to ∼7 deg close to the basal part. Some of the grooves, situated close to the gap between CS2 and CS1, were arranged parallel to this gap. The arrangement of the grooves in the ventro-lateral region of the claws showed a similar pattern, with the exception that the grooves nearly covered the whole segment towards the distal end of CS1.

CS2 was broader and more oval-shaped than CS1. The measured length was 394±32 µm (n=4). The base was 80±10 µm (n=4) wide, and the grooves found in the dorso-lateral and ventro-lateral regions of CS2 were not as prominent and large as those in CS1. Near the gap between CS1 and CS2, the grooves again ran parallel to the gap. The grooves were defined and clearly visible in the basal region of CS2, but became less defined towards the apical end. The overall arrangement of the grooves on CS2 was similar to that observed on CS1, but the grooves were of smaller size.

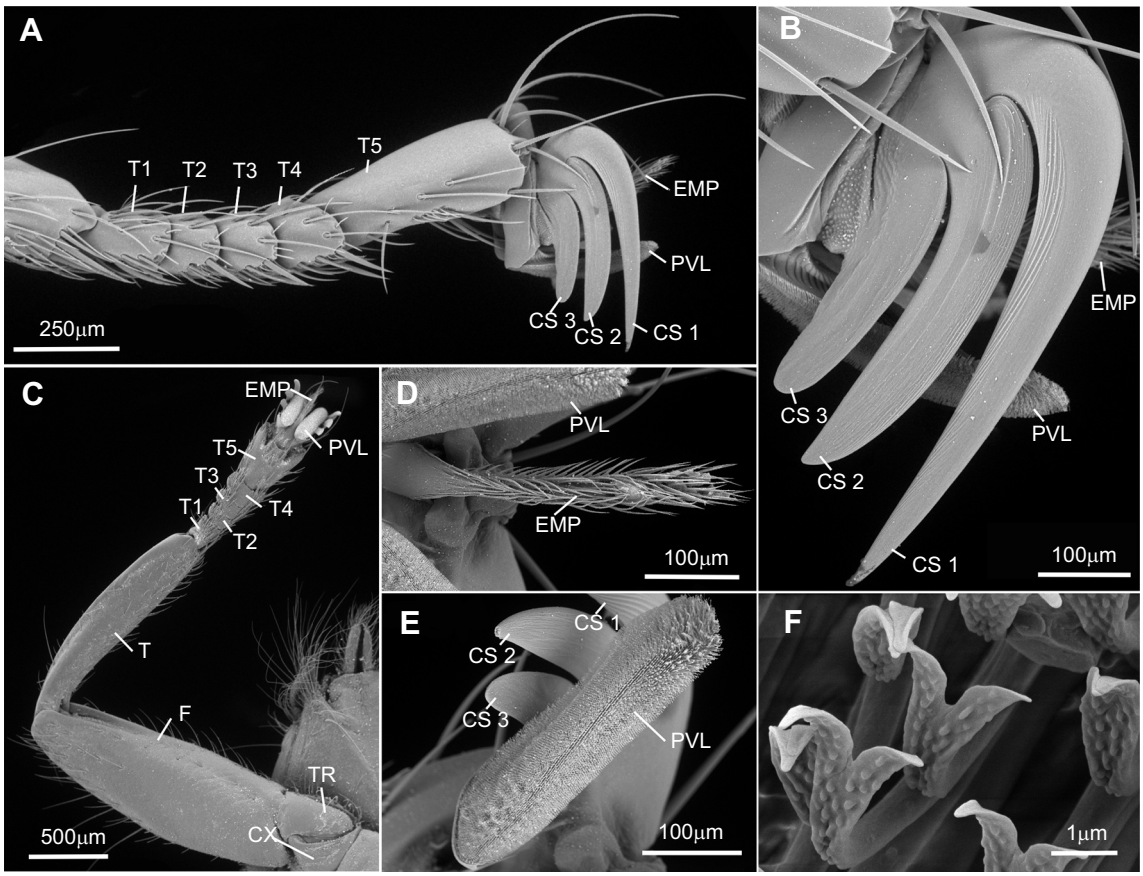

Fig. 2. Attachment system of *C. pallida*. Scanning electron microscopy (SEM) images. (A) Lateral overview of a front leg: the tarsus consists of five tarsomeres (T1–5) and the attachment system comprises a tridentate claw pair (claw segment CS1–3), pulvilli (PVL) and an empodium (EMP). (B) Detailed view of the tridentate claw with characteristic grooves on the outer side. (C) Ventral overview of the right front leg. CX, coxa; F, femur; T, tibia; TR, trochanter. (D) Detailed ventral view of the empodium. (E) Detailed ventral view of one pulvillus. (F) Detailed view of setae with dichotomous end structures located in the middle region of the pulvilli.

Journal of Experimental Biology (2018) 221, jeb179242. doi:10.1242/jeb.179242

CS3 was the smallest claw segment, with a length of 222±11 µm (n=4). The grooves were only located in the basal area close to the gap beside CS2 and were arranged similar to the apical areas of both CS2 and CS1.

The empodium, with a length of 490±6 µm, was located between the two pulvilli (n=4; Fig. 2D). It could be divided into a smooth proximal part with a length of 185±5 µm (n=4) and a structured distal part with a length of 316±12 µm (n=4) consisting of many bristle-shaped acanthae (Richards and Richards, 1979) with an average length of 45±23 µm (n=8) (Fig. 2C). The acanthae were pointed and either straight or slightly curved and were orientated in the distal direction with respect to the base of the empodium.

The pulvilli showed a rectangular shape (Fig. 2E). Close to the distal structured part of the empodium, the pulvilli were slightly curved. The foreleg pulvilli, with an area of ~35,500 µm^2 per pulvillus, were smaller than those at the middle legs, with an area of ~39,300 µm^2 per pulvillus, and the pads at the hindlegs, with an area of ~52,400 µm^2 per pulvillus (example measurement for one specimen as a rough approximation). Setal density on the legs was ~70 per 100 µm^2 (n=3). The setae had long narrow shafts and were orientated heterogeneously depending of their location on the pulvilli (Fig. 1F). In the middle section of each pulvillus from its proximal to distal end, setae were faced to the distal end of the pulvillus. The setae that were located in the middle region pointed towards the lateral margins of the pulvillus.

Terminal structures (spatulae) of individual setae were dichotomous and acuminated (Fig. 2E, Fig. 3E), except for those located at the very ends of the proximal and distal part of the pulvillus. Here, the end structures were one-headed and triangularly shaped (Fig. 3D). Compared with the setae in the middle region of the pad, those located at the outer margin of the pad were often fused at their bases. They formed thicker structures from which several setae arose. These fusions were absent from the lateral sites of the pad.

Analysis of attachment sites by cryo-SEM

In order to visualize attachment sites of setae on the host feathers, *C. pallida* individuals were immediately frozen after being attached to feathers (Fig. 3). At the first stage, the claws spread apart and moved into a downward position. During this motion, the apical tips of CS1 followed by CS2 and CS3 began to pierce the feather vane. The piercing led to a segregation of barbs and barbules (Fig. 3A,B). While the claws were continuously pushing downward, the barbules began to interlock within the tapered region between the single claw segments (Fig. 3A). By pulling the specimen in the caudal direction, the above-mentioned interlocking became stronger and the feathers themselves became fractured. In these cases, residues of feathers were observed in the tapered regions between the claw segments of *C. pallida*.

Like the prominent claws, the flexible pulvilli also moved in the downward direction during attachment (Fig. 3D). The dichotomous setae located on the ventral side of the pulvilli were bendable and were able to secure intimate contact to the feathers (Fig. 3E). We observed no direct contact between the feathers and the empodium during our cryo-SEM analysis.

CLSM analysis

The CLSM maximum intensity projection of the autofluorescence of an entire tarsus revealed a heterogeneous material composition. The colours used in Fig. 4 correspond to the following detected auto-fluorescence and, consequently, represent different material compositions: (1) blue represents regions consisting mainly of soft rubber-like protein (resilin); (2) red and orange represent regions dominated by sclerotized cuticle; (3) green and yellow represent regions dominating by chitin and small amounts of resilin. The more yellow, orange or red a region becomes, the more sclerotized it is.

Generally, the tarsomeres consisted of sclerotized cuticle, which was indicated by the red and yellow auto-fluorescence signal. The first three tarsomeres showed a surrounding resilin pad at their bases, indicated by the blue signal (Fig. 4). The same dark blue signal was found in the joint region of the fifth tarsomere, the most basal part of the attachment system (Fig. 4A,B), and in the joints between the pulvilli and pretarsus (Fig. 4C). The basal region of the claws, the pulvilli and the empodium appeared to be sclerotized (Fig. 4B,C). The claws themselves, as well as the setae on the tarsomeres, showed no auto-fluorescence and appeared black in the CLSM maximum intensity projection (Fig. 4A,B). The acanthae on

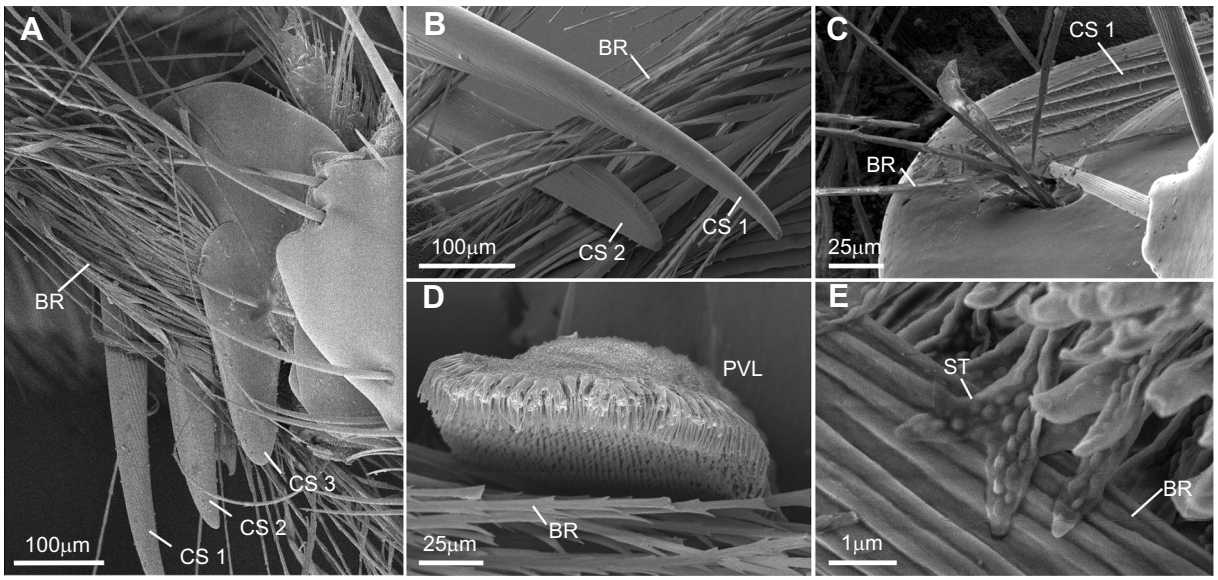

Fig. 3. Attachment process of *C. pallida* on feathers of *A. apus*. Cryo-SEM images. (A) Interlocking of the tridentate claw with feathers. BR, feather barbules; CS1–3, claw segments. (B) Detailed view of CS1 and CS2 penetrating feathers. (C) Interlocking with feather parts at the base of CS1–CS2. (D) Frontal view of the pulvillus (PVL) in contact with feathers. (E) Detailed view of one seta (ST) attached to a feather barbule (BR).

Journal of Experimental Biology (2018) 221, jeb179242. doi:10.1242/jeb.179242

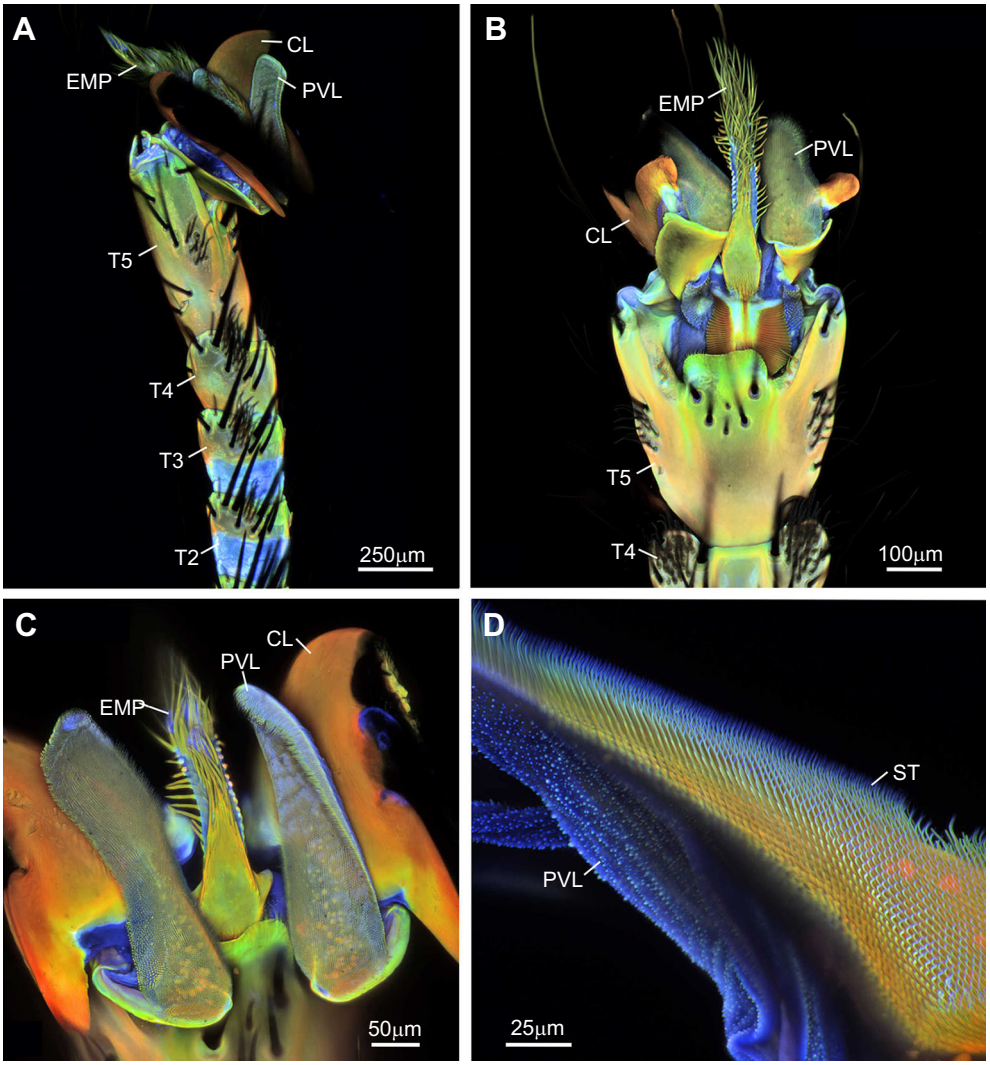

Fig. 4. Attachment system of *C. pallida*. Confocal laser scanning microscopy (CLSM) maximum intensity projection. (A) Lateral overview of the tarsus. T2–5, tarsomeres; EMP, empodium; PVL, pulvillus; CL, claw. (B) Ventral overview of the attachment system. (C) Detailed ventral view of the two pulvilli, claws and the empodium. (D) Detailed lateral view of one pulvillus at high magnification with adhesive setae (ST) on the ventral site.

the empodium showed a material gradient from their resilin-dominated blue base with first a green, chitin-dominated region followed by a more yellow–red region indicating stronger sclerotized cuticle (Fig. 4B,C). In contrast, adhesive setae located on the pulvilli showed a reverse material gradient, compared with the bristles. These setae bore resilin-dominating apical tips (blue signal) and a sclerotized base (yellow–red signal). The underlying cuticle of the pulvilli contained a high proportion of resilin, as it showed a strong blue fluorescence signal (Fig. 4D).

Friction force experiments

Data on males (n=20) and females (n=9) of *C. pallida* were pooled for further statistical analysis of the attachment force on the tested surfaces (Fig. 5). The results showed a significant influence of material (two-way ANOVA, P<0.01, n=29) and topography (surface orientation) (two-way ANOVA, P<0.01, n=29) on the maximum attachment force. We observed significantly higher attachment forces on surfaces with topography compared with the smooth surfaces regardless of their orientation (Holm–Sidak test, P<0.01). The louse flies showed the highest attachment forces when the saw teeth were orientated along the direction of locomotion, and the maximum attachment force was not significantly different with respect to the material (epoxy resin: 19.7±4.2 mN, silicone: 19.4±4.05 mN). The orientation of the saw teeth significantly influenced maximum attachment force only when they had been aligned laterally to the direction of the movement (Holm–Sidak test, P<0.01). There was a significant influence of material if the saw teeth were aligned laterally, but the maximum attachment forces were in a similar range between different materials (epoxy resin: 16.7±2.7 mN, silicone: 13.75±2.4 mN).

Crataerina pallida generated comparable maximum attachment forces on all surfaces (14–18 mN), except for smooth silicone (3.9±1.8 mN). Interestingly, during friction-force experiments, we observed strong sliding of fly individuals on the smooth silicone. However, maximum attachment forces were 15.4±2.7 mN on smooth epoxy resin and 15.2±3.2 mN on glass.

Detached single legs were used to estimate the potential attachment force on feathers. After bringing the tarsi into proper contact, we actively pulled legs with a micromanipulator. A single leg was able to withstand forces up to 324±26 mN (n=8) on feathers. However, we were not able to repeat the results after the first measurement. A light microscopy examination showed that parts of the pretarsus had fractured, while the claws remained attached to the feathers.

DISCUSSION

Attachment on feathers and the role of specialized claws

Based on our experimental observations, the modified claws of *C. pallida* seem to be primarily responsible for their extraordinary ability to reliably attach to feathers. During attachment of *C. pallida* to the plumage, the tridentate-like claws pierce the feather vane and

Journal of Experimental Biology (2018) 221, jeb179242. doi:10.1242/jeb.179242

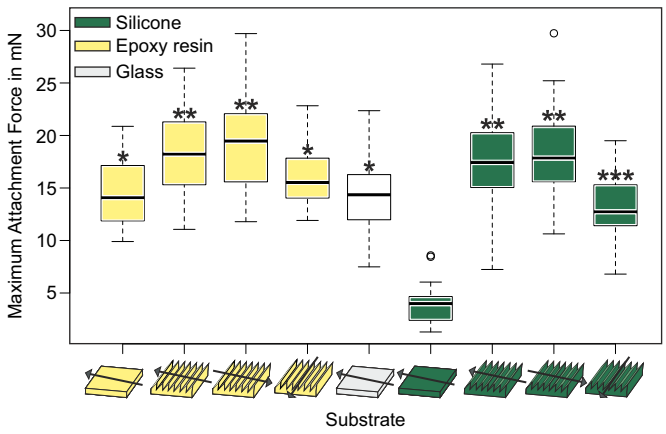

Fig. 5. Attachment experiments with *C. pallida* on different substrates. Maximum attachment forces measured on surfaces with saw teeth differ significantly from those on smooth substrates. The arrows indicate the orientation of the force applied on the insects while walking. Box plots show the median (black line), the lower and upper quartile (box) and the lower and upper 1.5 interquartile range (whiskers). Circles indicate outliers outside the 1.5 interquartile range. Groups with the same number of asterisks are statistically equal.

single barbs become lodged in the staggered base between individual spines of the claw (Fig. 3A). This clamping is enhanced by barbs and barbules slipping further and further into the tapered space between the spines towards their base, either by an active motion of the leg or by external load induced by the host itself. As a consequence, the normal load on the barbs is strongly increased, which in turn leads to high friction, preventing the pulling out of the barbs from the claw. The effect is further enhanced by the number of barbs lodged in the space of the claw, as well as by the presence of two potential 'clamping regions' between the three spines of each claw. A single detached leg is able to generate safety factors (SF, the maximal attachment force divided by the force of gravity of an individual insect) of up to 1000 with only four clamping regions (two left and two right). *Crataerina pallida* has six legs, resulting in a total of 24 clamping regions, making it literally impossible to detach without fracture of the substrate or the louse fly's legs. Also, once the barbs are firmly clamped, the orientation of the claws with respect to the barbs becomes unimportant, which, by implication, increases *C. pallida*'s manoeuvrability on the host.

We also conducted preliminary experiments on feathers and common dust napkins (data not shown), but the encountered forces were too high to measure with our experimental setup. Either the connection between the specimen and the force sensor broke or the substrate itself was torn apart. However, the fact that *C. pallida* is able to attach to dust napkins as well as it does on feathers of *A. apus*, at least in our experimental setup, implies that the functionality of the attachment system is not restricted to the host species or to feathers in general. It instead shows that such claws are well adapted to attach to any fibrillary surface or structure. Bush et al. (2006) obtained similar results with the mainly host-specific slender pigeon lice *Columbicula columbae*. They showed that the attachment strength does not correlate with feather size and attachment is equally efficient on feathers of different pigeon species. Interestingly, such friction-based principles, as for *C. pallida*'s attachment system, are common in other insect interlocking mechanisms; for instance, in the wing locking of beetles or in the head arresting system of dragonflies (Gorb et al., 2002). All these mechanisms are similar in being very energy efficient and not relying on additional strong muscle work. In conclusion, *C. pallida*'s attachment system may be able to attach to its host efficiently without great energy consumption, making it essential for the organism's success in its ecological niche.

Without a doubt, the enlarged, highly specialized claws are an important feature of *C. pallida*'s adaptations to its ectoparasitic lifestyle. Apart from Hippoboscidae, calyptrate flies normally have only single-tipped claws (Gorb, 2001; Wang et al., 2016). In this case, although the claws may be potentially able to interlock with the feather's base, single barbules may not be lodged in. The barbules are most likely going to bend as long as they are pulled. Because of this bending, the barbules will slip away from the claws, resulting in a very weak contact formation and overall attachment force. However, these so-called serrate or pectinate claws are not a unique feature of *C. pallida* or other hippoboscids, but have developed several times in the evolution of other arthropods. Such claws can be found in species that also attach to fibrillary surfaces in nature. For example, the orb web spider *Zygiella* (Araneae, Araneidae) has serrate claws to move on a spider web efficiently (Foelix, 1996). The fishing spider, *Dolomedes*, uses such claws to break its locomotion on the water surface by interlocking with its dragline (Gorb and Barth, 1994), the stick insect *Orthomeria* (Phasmatodea, Aschiphasmatidae) has pectinate claws and often encounters heterogeneous plant surfaces including some covered with trichomes (Vallotto et al., 2016), and the bee louse *Braula* (Diptera, Braulidae) has tiny comb-like claws to attach to hairs on the honey bee thorax (Ellis et al., 2010).

Attachment ability on smooth substrates

We performed friction-force experiments on surfaces varying in material and topography in order to further understand the functional mechanism of the attachment system of *C. pallida*. Smooth substrates were used to probe the attachment ability of the pulvilli. We initially assumed that the claws, because of their great enlargement, interfere with the louse fly's ability to attach to smooth substrates. However, our experiments revealed that, although the maximum attachment forces on the smooth surfaces are significantly different to the maximum attachment forces on the structured surfaces, the results are still in similar range, except for the smooth silicone control. The reduction of the maximum attachment force on smooth silicone by a factor of 0.74, compared with smooth epoxy resin and smooth glass, is in line with previous results gathered on the ladybird beetle *Coccinella septempunctata* (Coleoptera, Coccinellidae) and may be explained by a different interfacial stress distribution of setae on soft substrates compared with stiff ones (Heepe et al., 2016). A comparison of the safety factors with those from previous experiments on smooth substrates reveals that, in conflict with our initial assumption, *C. pallida* attaches even better to smooth substrates than other Brachycera. *Crataerina pallida*'s safety factor is at least three times higher (SF ~90) than that of two syrphid flies with similar weight measured on PVC (*Sphaerophoria scripta* SF ~30 and *Episyrphus balteatus* SF ~25; Gorb et al., 2001). It is worth mentioning that the attachment ability of both syrphid flies was measured passively in a centrifuge while *C. pallida*'s attachment ability was measured actively by the insect pulling on its own. Therefore, the maximum attachment ability measured for *C. pallida* is restricted to the animal's musculature and may be even higher if measured in a centrifuge.

Crataerina pallida's high safety factor on smooth surfaces indicates that they also have to attach to other heterogeneous

Journal of Experimental Biology (2018) 221, jeb179242. doi:10.1242/jeb.179242

surfaces, including smooth ones. After hatching, *C. pallida* is located in the nests of *A. apus* and may encounter relatively smooth and sometimes soft surfaces like egg shells, young naked nestlings still without feathers or plant residues (Weitnauer, 1947). Also, the nest hole itself may consist of various materials including wood, concrete or stone. Our morphological analysis showed differences in the architecture of pulvilli in *C. pallida*, when compared with that of the two syrphid flies mentioned above and the more closely related calyptrates. Normally, Brachycera have a non-serrate, single-tipped pair of claws and pulvilli with setae having single-tipped spatulae. These setae are usually used to attach to smooth surfaces (Niederegger et al., 2002; Varenberg et al., 2010). Reliable attachment is only possible if the setae can get in proper contact, leading to a sufficient real contact area between them and the substrate (Persson, 2003). *Crataerina pallida*'s pulvilli consist of dichotomously shaped setae in a very high density with around 70 setae per 100 µm². In comparison with that of other calyptrate flies of the same dimension and having similar pulvilli sizes, the setal density in *C. pallida* is more than twice as high: *Calliphora calliphoroides* ∼14 setae per 100 µm², *Muscina stabulans* ∼19 setae per 100 µm², *Lucilia sericata* ∼38 setae per 100 µm² (Wang et al., 2016).

Dichotomously shaped setae have also been found in the beetle *Hemisphaerota cyanea* (Chrysomelidae; Cassidinae; Eisner and Aneshansley, 2000). The beetle is able to endure strong pulling forces and to use this enhanced attachment as a defensive mechanism against predation. The appearance of such setae may not be coincidental in *C. pallida*, because it is known that splitting of the contact area greatly enhances possible attachment abilities (Arzt et al., 2003; Varenberg et al., 2010). This may allow it to compensate for the claw's possible disturbance during contact formation, as a small part of the pulvilli being in proper contact may provide sufficient attachment for relatively light flies.

Apart from the external morphology, the material composition, especially the occurrence of resilin in certain structures, is important for the functionality of an attachment system. The elastic protein resilin (Weis-Fogh, 1960) is known for its high resilience, low fatigue and strong damping (see review by Michels et al., 2016). We show, for the first time, that the material (sclerotization) gradient of the setae previously reported for *Coccinella septempunctata* (Peisker et al., 2013) is also present in a species within the order Diptera. A proper contact between setae and the surface is necessary to generate strong attachment forces. Therefore, a biological system needs on the one hand a certain flexibility of the involved microstructures to compensate for varying roughness and on the other hand a certain stiffness as well as mechanical stability to generate sufficient attachment forces. The observed material gradient of the setae with a soft tip and a stiff base improves the function of the attachment system considerably by enabling effective contact formation while preventing collapse and clustering of the setae (Peisker et al., 2013; Gorb and Filippov, 2014).

Attachment ability on structured substrates

Structured surfaces were used to mainly probe the interlocking ability of the claws with the substrate. The first striking results are that the overall maximum attachment forces were higher on structured surfaces than on smooth surfaces regardless of orientation and, contrary to the results obtained from smooth samples, the maximum attachment force was almost independent of the material stiffness. This independence of maximum attachment force with respect to stiffness indicates that sufficient interlocking takes place on both soft and stiff substrates and that stiffness overall plays only a marginal role. We further observed significantly higher attachment forces on surfaces with saw teeth aligned along or against the pulling direction compared with laterally aligned saw teeth or smooth surfaces. Interestingly, maximum attachment force was not significantly different between experimental situations when the claws interlock with saw teeth that are orientated along or against the pulling direction. However, the maximum attachment force was on average higher with saw teeth orientated along the pulling direction on both substrates. These results may be explained by synergistic effects between claws and pulvilli during attachment (Fig. 6A,B). If the pulling direction of the legs is aligned against the saw teeth, the pulvilli are not able to build up a large contact area with the substrate because of interference with claws that are responsible for strong attachment (Fig. 6A). If the pulling direction is aligned along the saw teeth, the pulvilli may be able to come into contact with the surface, which then results in an overall strong attachment force (Fig. 6B).

The maximum attachment forces were significantly reduced on laterally aligned saw teeth compared with the other two orientations. This reduction may occur because it is more difficult for the claws to interlock with the structure properly. Again, no big influence of stiffness could be observed, and *C. pallida* was even able to attach to laterally aligned saw teeth in a manner which still exceeded the maximum attachment force of the syrphid flies mentioned above (Gorb et al., 2001). In particular, comparison of the laterally aligned

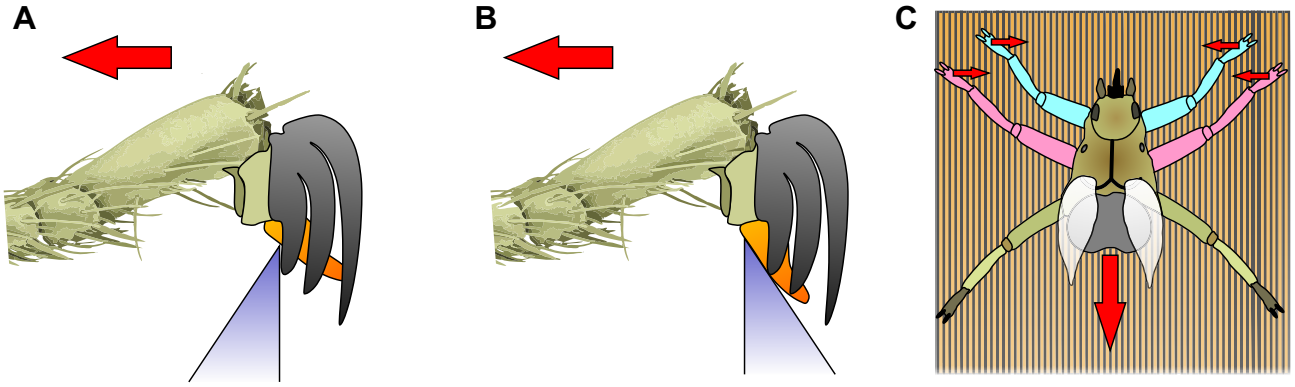

Fig. 6. Schematic diagram of contact formation on surfaces with saw teeth. (A) Interlocking on saw teeth aligned against the pulling direction (red arrow). Claws are shown in grey and pulvilli in orange. (B) Interlocking on saw teeth aligned along the pulling direction. (C) Orientation of the legs on saw teeth aligned laterally to the pulling direction. The position of the front legs (light blue) and the middle legs (pink) is highlighted. Applied forces are highlighted by red arrows.

saw teeth and the smooth substrate made up of soft material highlights the overall importance of the claws during attachment on structured surfaces, as the maximum attachment was increased by 0.72 on laterally aligned saw teeth.

We observed changes in the leg positions as soon as *C. pallida* walked on laterally aligned saw teeth, when compared with walking on saw teeth aligned along or against the pulling direction (Fig. 6C). In the latter case, *C. pallida*'s middle and forelegs were orientated in the cranial direction while the hindlegs were orientated in the caudal direction. On laterally aligned saw teeth, the middle and forelegs reorientated themselves in such a way that the tarsi and the claws specifically were perpendicularly oriented to the saw teeth (Fig. 6C). By doing so, *C. pallida* may increase the normal load of the claw tips to the saw teeth, and also the resulting friction force by actively pulling the legs towards the thorax. Possible adaptations in walking behaviour, depending on surface roughness or ceiling walk, have been reported in different insects. For instance, Hosoda and Gorb (2011) have shown that the green dock beetle, *Gastrophysa viridula*, shows frequent grooming behaviour when walking on rough substrates and the housefly *Musca domestica* changes its horizontal walking gait pattern as soon as it walks on the ceiling, in order to provide an optimal relationship between body weight and contact configuration (Gorb and Heepe, 2018).

We noticed that *C. pallida* did not always walk in a modified tripod gait pattern known for other insects (Wilson, 1966) on our tested surfaces. Prior to walking, *C. pallida* sometimes showed an indistinct, tapping movement with their legs which can also be observed in its natural environment. During this tapping movement, the legs were kept at full stretch most of the time, and the whole body stayed close to the substrate. The function of this behaviour remains unknown, but the tapping could represent an active probing for sufficient attachment strength.

The role of the empodium

The empodium has bristle-shaped extensions and may work as a counterpart to the claws. Because of its comb-like structure, we first assumed that the empodium may be capable to interlock with the feathers and pull them towards the claws more effectively. However, we cannot confirm this function based on our observations using cryo-SEM. No cases were observed in which the empodium was interlocked with the feathers. Therefore, we suggest here that no immediate contribution by the empodium to the attachment occurs. Nonetheless, the empodium may have an important role in retaining the function of the attachment system. Residues of feathers between the tapered regions of the claw segments or clustering of the setae on the pulvilli may compromise the attachment ability (Fig. 3C). We hypothesize that the empodium may act as a cleaning device during grooming. The bristles on the empodium are tapered in the apical direction and may be able to clean the tapered regions of the claw segments and return the setae to an un-clustered state. Strong forces might be present during the grooming process, because we observed strong destruction on the empodium with sometimes completely missing bristles in living flies. The soft and elastic resilin joints at the bristle's base observed by CLSM may have developed to increase the resilience and longevity of the empodium's bristles, similar to the flexible mounting of sharkskin scales in the tissue, preventing damage of the interlocked microstructures (Manoonpong et al., 2016).

Acknowledgements

We would like to thank Ilka Kureck for providing images of living louse flies.

Competing interests

The authors declare no competing or financial interests.

Author contributions

Conceptualization: D.S.P., S.N.G.; Methodology: D.S.P., N.K., S.N.G.; Validation: L.H.; Formal analysis: D.S.P., N.K.; Investigation: D.S.P., N.K., L.H., S.B.; Resources: N.K., A.H.W., K.W.; Writing - original draft: D.S.P., N.K.; Writing - review & editing: L.H., S.B., A.H.W., K.W., S.N.G.; Visualization: D.S.P., L.H., S.B.; Supervision: L.H., S.N.G.; Project administration: D.S.P.

Funding

S.B. acknowledges financial support from the German Science Foundation (Deutsche Forschungsgemeinschaft; BU3169/1–1).

References

Arzt, E., Gorb, S. N. and Spolenak, R. (2003). From micro to nano contacts in biological attachment devices. *Proc. Natl Acad. Sci. USA* **100**, 10603-10606.
Bequaert, J. C. (1953). The Hippoboscidae or louse-flies (Diptera) of mammals and birds. Part I. Structure, physiology and natural history. *Entomol. Am.* **33**, 211-442.
Beutel, R. G. and Gorb, S. N. (2001). Ultrastructure of attachment specializations of hexapods (Arthropoda): evolutionary patterns inferred from a revised ordinal phylogeny. *J. Zool. Syst. Evol. Res.* **39**, 177-207.
Bullock, J. M. R. and Federle, W. (2011). The effect of surface roughness on claw and adhesive hair performance in the dock beetle *Gastrophysa viridula*. *Insect Sci.* **18**, 298-304.
Bush, S. E., Sohn, E. and Clayton, D. H. (2006). Ecomorphology of parasite attachment: experiments with feather lice. *J. Parasitol.* **92**, 25-31.
Dai, Z., Gorb, S. N. and Schwarz, U. (2002). Roughness-dependent friction force of the tarsal claw system in the beetle *Pachnoda marginata* (Coleoptera, Scarabaeidae). *J. Exp. Biol.* **205**, 2479-2488.
Eisner, T. and Aneshansley, D. J. (2000). Defense by foot adhesion in a beetle(*Hemisphaerota cyanea*). *Proc. Natl Acad. Sci. USA* **97**, 6568-6573.
Ellis, J. D., Mortensen, A. N. and Zettel Nalen, C. M. (2010). http://entnemdept.ufl.edu/creatures/misc/bees/bee_louse.htm accessed: 24. 11. 2017.
Foelix, R. F. (1996). *Biology of Spiders*, 2nd edn. New York: Oxford University Press.
Friedemann, K., Schneeberg, K. and Beutel, R. G. (2014). Fly on the wall–attachment structures in lower Diptera. *Syst. Entomol.* **39**, 460-473.
Gorb, S. N. (1998). The design of the fly adhesive pad: distal tenent setae are adapted to the delivery of an adhesive secretion. *Proc. R. Soc. B* **265**, 747-752.
Gorb, S. N. (2001). *Attachment Devices of Insect Cuticle*. Dordrecht: Kluwer.
Gorb, S. N. and Barth, F. G. (1994). Locomotor behavior during prey-capture of a fishing spider, *Dolomedes plantarius* (Araneae: Araneidae): galloping and stopping. *J. Arachnol.* **22**, 89-93.
Gorb, S. N. and Filippov, A. E. (2014). Fibrillar adhesion with no clusterisation: functional significance of material gradient along adhesive setae of insects. *Beilstein J. Nanotechnol.* **5**, 837-845.
Gorb, E. V. and Gorb, S. N. (2002). Attachment ability of the beetle *Chrysolina fastuosa* on various plant surfaces. *Entomol. Exp. Appl.* **105**, 13-28.
Gorb, E. V. and Gorb, S. N. (2009). Effects of surface topography and chemistry of *Rumex obtusifolius* leaves on the attachment of the beetle *Gastrophysa viridula*. *Entomol. Exp. Appl.* **130**, 222-228.
Gorb, E. V. and Gorb, S. N. (2011). The effect of surface anisotropy in the slippery zone of *Nepenthes alata* pitchers on beetle attachment. *Beilstein J. Nanotechnol.* **2**, 302-310.
Gorb, S. N. and Heepe, L. (2018). Biological fibrillar adhesives: functional principles and biomimetic applications. In *Handbook of Adhesion Technology* (ed. L. da Silva, A. Öchsner and R. Adams), Cham: Springer.
Gorb, S. N., Gorb, E. V. and Kastner, V. (2001). Scale effects on the attachment pads and friction forces in syrphid flies (Diptera, Syrphidae). *J. Exp. Biol.* **204**, 1421-1431.
Gorb, S. N., Beutel, R. G., Gorb, E. V., Jiao, Y., Kastner, V., Niederegger, S., Popov, V. L., Scherge, M., Schwarz, U. and Vötsch, W. (2002). Structural design and biomechanics of friction-based releasable attachment devices in insects. *Integr. Comp. Biol.* **42**, 1127-1139.
Gorb, E. V., Haas, K., Henrich, A., Enders, S., Barbakadze, N. and Gorb, S. N. (2005). Composite structure of the crystalline epicuticular wax layer of the slippery zone in the pitchers of the carnivorous plant *Nepenthes alata* and its effect on insect attachment. *J. Exp. Biol.* **208**, 4651-4662.
Gorb, S. N., Schuppert, J., Walther, P. and Schwarz, H. (2012). Contact behaviour of setal tips in the hairy attachment system of the fly Calliphora vicina (Diptera, Calliphoridae): a cryo-SEM approach. *Zoology* **115**, 142-150.
Heepe, L., Petersen, D. S., Tölle, L., Wolff, J. O. and Gorb, S. N. (2016). Sexual dimorphism in the attachment ability of the ladybird beetle *Coccinella septempunctata* on soft substrates. *Appl. Phys. A.* **123**, 34.
Hosoda, N. and Gorb, S. N. (2011). Friction force reduction triggers feet grooming behavior in beetles. *Proc. R. Soc. B* **278**, 1748-1752.

Hutson, A. M. (1981). The population of the louse-fly, *Crataerina pallida* (Diptera, Hippoboscidae) on the European swift, *Apus apus* (Aves, Apodidae). *J. Zool. Lond.* **194**, 305-316.
Kemper, H. (1951). Beobachtungen an *Crataerina pallida* Latr. und *Melophagus ovinus* L. (Diptera, Pupipara). *Zeitschrift für Hygiene (Zoologie)* **39**, 225-259.
Langer, M. G., Ruppersberg, J. P. and Gorb, S. N. (2004). Adhesion forces measured at the level of a terminal plate of the fly's seta. *Proc. R. Soc. B* **271**, 2209-2215.
Lee, P. L. and Clayton, D. H. (1995). Population biology of swift (*Apus apus*) ectoparasites in relation to host reproductive success. *Ecol. Entomol.* **20**, 43-50.
Manoonpong, P., Petersen, D. S., Kovalev, A., Wörgötter, F., Gorb, S. N., Spinner, M. and Heepe, L. (2016). Enhanced locomotion efficiency of a bio-inspired walking robot using contact surfaces with frictional anisotropy. *Sci. Rep.* **6**, 39455.
Marshall, A. G. (1981). *The Ecology of Ectoparasitic Insects*. London: Academic Press Inc.
Michels, J. and Gorb, S. N. (2012). Detailed three-dimensional visualization of resilin in the exoskeleton of arthropods using confocal laser scanning microscopy. *J. Microsc.* **245**, 1-16.
Michels, J., Appel, E. and Gorb, S. N. (2016). Functional diversity of resilin in Arthropods. *Beilstein J. Nanotechnol.* **7**, 1241-1259.
Niederegger, S. and Gorb, S. N. (2003). Tarsal movements in flies during leg attachment and detachment on a smooth substrate. *J. Insect Physiol.* **49**, 611-620.
Niederegger, S., Gorb, S. N. and Jiao, Y. (2002). Contact behavior of tenent setae in attachment pads of the blowfly *Calliphora vicina* (Diptera, Calliphoridae). *J. Comp. Physiol. A* **187**, 961-970.
Oldroyd, H. (1966). The wing of *Crataerina pallida* (Latreille) (Diptera: Hippoboscidae). *Syst. Entomol.* **35**, 23-25.
Peisker, H., Michels, J. and Gorb, S. N. (2013). Evidence for a material gradient in the adhesive tarsal setae of the ladybird beetle *Coccinella septempunctata*. *Nat. Commun.* **4**, 1661.
Peressadko, A. G. and Gorb, S. N. (2004). Surface profile and friction force generated by insects. In *First International Industrial Conference Bionik* (ed. I. Boblan and R. Bannasch), pp. 257-261. Düsseldorf: VDI Verlag.
Persson, B. N. J. (2003). On the mechanism of adhesion in biological systems. *J. Chem. Phys.* **118**, 7614-7621.
Richards, A. G. and Richards, P. A. (1979). The cuticular protuberances of insects. *Int. J. Insect Morphol. Embryol.* **8**, 143-157.
Song, Y., Dai, Z., Wang, Z., Ji, A. and Gorb, S. N. (2016). The synergy between the insect-inspired claws and adhesive pads increases the attachment ability on various rough surfaces. *Sci. Rep.* **6**, 26219.
Spurr, A. R. (1969). A low-viscosity epoxy resin embedding medium for electron microscopy. *J. Ultrastruct. Res.* **26**, 31-43.
Stork, N. E. (1980). Experimental analysis of adhesion of *Chrysolina polita* (Chrysomelidae: Coleoptera) on a variety of surfaces. *J. Exp. Biol.* **88**, 91-108.
Stork, N. E. (1983a). A comparison of the adhesive setae on the feet of lizards and arthropods. *J. Nat. Hist.* **17**, 829-835.
Stork, N. E. (1983b). The adherence of beetle tarsal setae to glass. *J. Nat. Hist.* **17**, 583-597.
Tompkins, D. M., Jones, T. and Clayton, D. H. (1996). Effect of vertically transmitted ectoparasites on the reproductive success of swifts (*Apus apus*). *Funct. Ecol.* **10**, 733-740.
Tramsen, H. T., Gorb, S. N., Zhang, H., Manoonpong, P., Dai, Z. and Heepe, L. (2018). Inversion of friction anisotropy in a bio-inspired asymmetrically structured surface. *J. R. Soc. Interface* **15**.
Vallotto, D., Bresseel, J., Heitzmann, T. and Gottardo, M. (2016). A black-and-red stick insect from the Philippines–observations on the external anatomy and natural history of a new species of Orthomeria. *ZooKeys* **559**, 35-57.
Varenberg, M., Pugno, N. M. and Gorb, S. N. (2010). Spatulate structures in biological fibrillar adhesion. *Soft Mat.* **6**, 3269-3272.
Voigt, D., Schuppert, J. M., Dattinger, S. and Gorb, S. N. (2008). Sexual dimorphism in the attachment ability of the Colorado potato beetle *Leptinotarsa decemlineata* (Coleoptera: Chrysomelidae) to rough substrates. *J. Insect Physiol.* **54**, 765-776.
Wang, Q. K., Yang, Y. Z., Li, X. Y., Li, K. and Zhang, D. (2016). Comparative ultrastructure of pretarsi in five calyptrate species. *Parasitol. Res.* **115**, 2213-2222.
Weis-Fogh, T. (1960). A rubber-like protein in insect cuticle. *J. Exp. Biol.* **37**, 889-907.
Weitnauer, E. (1947). Am Neste des Mauerseglers, *Apus apus (L.). Ornithol. Beob.* **44**, 133-182.
Whitten, J. M. (1969). Coordinated development in the fly foot:sequential cuticle secretion. *J. Morphol.* **127**, 73-104.
Wilson, D. M. (1966). Insect walking. *Annu. Rev. Entomol.* **11**, 103-122.